Applied Geochemistry 86 (2017) 36–48

Contents lists available at ScienceDirect

Applied Geochemistry

journal homepage: www.elsevier.com/locate/apgeochem

Sorption of radium onto early cretaceous clays (Gault and *Plicatules* Fm). Implications for a repository of low-level, long-lived radioactive waste

Tiziana Missana [a], Elisenda Colàs [b], Fidel Grandia [b], Javier Olmeda [b], Manuel Mingarro [a], Miguel García-Gutiérrez [a], Isabelle Munier [c], Jean-Charles Robinet [c], Mireia Grivé [b, *]

[a] CIEMAT, Department of Environment, Av. Complutense, 40, 28040 Madrid, Spain
[b] Amphos21 Consulting S.L., Pg. Garcia-Fària 49, 08019 Barcelona, Spain
[c] Andra, R&D Division, 1-7 rue Jean Monnet, 92298 Châtenay-Malabry, France

ARTICLE INFO

Article history:
Received 8 April 2017
Received in revised form
14 July 2017
Accepted 13 September 2017
Available online 19 September 2017

Handling Editor: Prof. M. Kersten

Keywords:
Radium
Clay
Sorption
LL-LL waste

ABSTRACT

The repository of low-level and long-lived radioactive waste from REE purification and treatment is presently under investigation by the French National Radioactive Waste Management Agency (Andra). This waste consists of Ra-bearing solids, mainly Ra-barite (Ba,Ra)(SO_4), along with other salts such as NH_4NO_3 and monazite. The current repository concept under study is based on a shallow (~30 m deep) geological disposal in a clay formation. This work deals with the experimental study of the sorption of Ra onto two clay rocks from Lower Cretaceous geological formations in the Department of Aube, in France, the Gault (*tégulines*) Formation and *Plicatules* Formation.

Clay samples were extracted from different boreholes from the both geological clay formations, and consisted mainly of illite, illite-smectite mixed layers (35–65% and 25–70%). Sorption experiments were carried out on raw materials as well as on samples exchanged with different cations (homoionic forms of Na, NH_4, Ba and Ca, respectively). The results indicate that Ra sorption in raw materials is linear within the range of concentration investigated (10^{-8} - 10^{-11} M). In most of the samples, K_d values from 170 to 300 g·mL^{-1} were measured for Ra and from 30 to 70 g·mL^{-1} for Ba. The sorption experiments (from 1 h to 92 days) of Ra showed small kinetic effects as K_d values tend to increase with time from approximately logK_d = 2.15 to 2.65. In all exchanged samples, a dependence of sorption on the ionic strength was observed -the higher the ionic strength, the lower K_d values-; except for Na, this dependence is consistent with an ionic exchange process and selectivity coefficients (Ra-Ca; Ra-Ba and Ba-Ca) have been determined. A non-negligible effect of pH on sorption was also observed that could be explained considering surface complexation on the amphoteric groups present at the solid surface. In these materials, the selectivity of Ra was higher than that of Ba (half an order of magnitude).

The experimental results indicate that sorption of Ra in the studied clay formations is high enough to limit the radium migration in the near field of a low-level, long lived disposal site.

1. Introduction

Radium-bearing waste comes from uranium ore mining and milling, the treatment of groundwaters from deep geological formations, oil production or industrial activities and from the spent fuel in nuclear energy plants. In some industrial activities, such as the production of rare earths elements (REE's), the waste consists of Ra-bearing solids, basically Ra- barite, (Ba,Ra)(SO_4), along with other salts such as NH_4NO_3 and monazite. In general, radioactivity of radium-bearing waste is low to intermediate level (up to some hundreds of Bq·g^{-1}) but this waste contains a significant amount of long-lived radionuclides in addition to radium-226. The French national radioactive waste management agency (Andra) has been studying a repository concept for radium bearing waste based on a shallow (~20–30 m deep) geological disposal in a clay-rich sedimentary formation.

Radium is an alkaline earth and this group of elements has

* Corresponding author.
E-mail address: mireia.grive@amphos21.com (M. Grivé).

https://doi.org/10.1016/j.apgeochem.2017.09.009
0883-2927/

strong affinity with exchange sites in clay minerals such as montmorillonite and illite (Tachi et al., 2001; Missana et al., 2008); therefore, sorption could be a key geochemical process for the retention of Ra released from the waste. Sorption data of radium onto clay minerals and rocks are presently very scarce in literature and most of the information comes from analogue elements such as barium and strontium. Furthermore, the presence of highly soluble salts in the waste would lead to the release of cations such as NH_4^+ that would compete for sorption with Ra; however, data on NH_4^+ effect on radium retention in natural clays are nearly inexistent. New data on natural clay formations are needed to evaluate the migration of radium through the geological host-formation and support Performance Assessment of a radium-bearing waste repository hosted in a clay-rich sedimentary formation.

In this paper, an experimental study of the sorption of Ra onto the Gault Fm and *Plicatules* Fm (Lower Cretaceous, Department of Aube, France) is reported. These sedimentary formations are under study by Andra for hosting a Ra-waste repository site in France. Sorption experiments have been performed using (1) raw materials and (2) pre-treated, exchanged clays. The objective of the work is the determination of the Ra capacity to sorb/exchange onto clays and the effect of a number of parameters such as pH, solid-to-liquid ratio and ionic strength on the retention. The use of pre-treated clay allows the determination of the impact of ion competition on sorption. Furthermore, the selectivity and half-reaction constants have been calculated and compared to data available in literature. Also, the data obtained have been compared to Ba sorption data under the same experimental conditions to determine if this element could be further used as analogue.

2. Background of sorption of Ra and other alkaline earths onto clays

Data on Ra sorption on clay-rich materials, in particular for natural clay-rich media, are scarce in literature since experiments with radioactive material require especial procedures and materials to ensure workers protection. Only few previous investigations have been performed to date. Among them, Ames et al. (1983a, b) studied the sorption of radium onto different clay materials in 0.01 M NaCl solutions. They determined Ra sorption for a number of clay minerals, and determined the following sequence of sorption affinities: clinoptilolite > nontronite > glauconite > montmorillonite > kaolinite. The authors concluded that sorption efficiency is correlated with cation-exchange capacity, and, therefore, the most efficient Ra sorbents were those clay minerals with the highest cation-exchange capacities, with the notable exception of montmorillonite. The authors also suggested that the differences observed between montmorillonite and nontronite, both dioctahedral smectites, may indicate that nontronite is a much more efficient sorbent for radium than montmorillonite due to the predominant tetrahedral charge exhibited by nontronite. Although the ion-exchange was suggested to be the most likely retention mechanism, the authors noticed that distribution coefficients generally decreased with increasing Ra concentration (in the range $5{\cdot}10^{-9}$ to $5{\cdot}10^{-7}$ M).

Tachi et al. (2001) carried out sorption and diffusion experiments in bentonite (mainly composed by smectite, 46–49%, and quartz/chalcedony, 38–39%) at different pH, ionic strength and S/L ratios. The determined sorption coefficients were in the range of 10^2–10^4 mL g^{-1}, depending on ionic strength and pH of the samples. These authors concluded that sorption of Ra on bentonite was dominated by ion exchange on smectite, and the observed apparent pH dependence of sorption was related to changes in Ca concentration from dissolution and precipitation of calcite.

Finally, Tamamura et al. (2014) studied the dependence of Ra adsorption on montmorillonite and kaolinite on salinity. The measured distribution coefficients decreased from $\approx 10^4$ to ≈ 100 mL g^{-1} with increasing NaCl concentration (from 0.01 to 1 M NaCl). At lower NaCl concentrations (<0.5 M), the distribution coefficients were higher for montmorillonite than for kaolinite. This behaviour is in agreement with the CEC of the studied clay minerals, which is higher for montmorillonite (82.3 mmol·100 g^{-1}) than for kaolinite (3.1 mmol·100 g^{-1}). At higher NaCl concentration (>0.5 M) the distribution coefficients for montmorillonite were equal to or lower than kaolinite distribution coefficients. The authors suggested that this behaviour was related with the higher negative charge density of montmorillonite. It was concluded that both CEC and crystal lattice of the clay minerals influenced the dependence of Ra adsorption with salinity.

Other alkaline earth elements such as Ba and Sr are expected to behave in a similar way as Ra when interacting with clay interlayers or external surfaces so it has been traditionally proposed that they can be considered as Ra analogues. A much larger number of sorption experiments with these cations have been carried out (Zhang et al., 2001; Missana and García-Gutierrez, 2007; Missana et al., 2008; Vilks et al., 2011). However, despite sharing geochemical properties, no definitive comparison between the sorption behaviour of these elements and Ra has been established.

3. Materials and methods

3.1. Clays

Clay samples came from the lower part of the Albian Gault clay Formation (locally called *tégulines clays*) and the lower Aptian *Plicatules* Formation located in the eastern part of the Paris Basin (Departement of Aube). These sedimentary clay-rich formations have been considered of interest by Andra for hosting a disposal facility of radium-bearing radioactive waste. Samples were extracted from different boreholes performed during a geological campaign and selected for sorption experiments (Table 1). The drill cores were sealed in aluminium bags on-site and opened in the laboratory in an anaerobic glove box. Part of the material was manually crushed in an agate mortar and the grinded materials were screened in ASTM sieves of 100 μm. All these procedures were carried out in the glove box under N_2+CO_2 (1%) atmosphere.

From the mineralogical point of view, Gault formation consists of 35–65% of illite, illite-smectite mixed layers and kaolinite. Quartz is found from 20% to 60% and carbonates, mainly calcite, are less than 30%). The *Plicatules* formation is made up of clay minerals around 25–70%, mainly illite, illite-smectite mixed layers and kaolinite. Quartz is found in variable amounts from 20% to 65% and carbonates less than 10%.

Sorption experiments were carried out on the raw materials and also on samples after exchange with different cations. The clay from the Gault formation (Sample 1) was converted into four homoionic forms (Na, NH_4, Ba and Ca) using 10 g of the raw material suspended in 300 mL of the respective electrolyte (1 mol L^{-1} of $NaClO_4$, NH_4ClO_4, $Ba(ClO_4)_2$ or $Ca(ClO_4)_2$). The suspensions were stirred overnight and then decanted; the process was repeated 4 times.

Table 1
Samples selected for sorption experiments.

Name	Sample, borehole, depth (m)	Formation
Sample 1	AUB01091 AUB121 59.8	Gault
Sample 3	AUB01064 AUB121 48.47	Gault
Sample 8	AUB00504 AUB161 27.45	Plicatules
Sample 9	AUB00811 AUB141 15.15	Gault
Sample 15	AUB00658 AUB151 26.8	Gault

After the last decantation, the solid was washed with deionized water and centrifuged/decanted several times until the electrical conductivity (EC) measured in the suspension was lower than 150 $\mu S \cdot cm^{-1}$. The EC was measured using a Crison EC-meter Basic 30. Calibration of the conductivity cell was made with standards of 213 $\mu S \cdot cm^{-1}$, 1413 $\mu S \cdot cm^{-1}$ and 12.88 $mS \cdot cm^{-1}$ at 25 °C.

At the end of the procedure, the exchanged samples were dried in the oven at 70 °C during 48–72 h and finally crushed in an agate mortar. Then the samples were re-suspended in the respective electrolyte at the desired ionic strength and solid-to-liquid (S/L) ratio (1 or 10 g L^{-1}).

3.2. Preparation of the synthetic gault water (SGW)

Synthetic pore water, representative of the Gault Formation porewater (SGW), was prepared for sorption experiments. Water preparation was performed in an oxygen-free glove box with a controlled atmosphere ($pCO_2 = 1 \cdot 10^{-2}$ atm., given by 99.9% N_2 and 1% CO_2). Those conditions are similar to the ones expected *in-situ* (Gaucher et al., 2009).

The deionized water (Grade I) used to prepare the suspensions was boiled for at least 15 min to minimize CO_2 contamination. The preparation was performed at room temperature (22 ± 3 °C), and then the synthetic water was stored into the glove box in dark bottles. After the addition of all the salts, the solution was filtered by a pore membrane of 0.1 μm to eliminate traces of eventual precipitates.

The chemistry of the SGW is detailed in Table 2. Chemical analyses were carried out by ICP-AES (Inductively Coupled Plasma Atomic Emission Spectrometry) and FAAS (Flame Atomic Absorption Spectrometry). The uncertainty of these measurements is less than 5%.

In order to verify if solid-water interactions could affect water chemistry during sorption experiments, the analysis of the synthetic water and pure electrolytes was carried out after being in contact with the solids. The aqueous phase was mixed with the solid at different solid-to-liquid ratios (1–10 g/L) and maintained in continuous stirring during the selected time. The separation of the supernatant from the solid was carried out by filtration (100 nm) or ultra-centrifugation (645000×*g*). The concentration of different monovalent cations (K^+, Na^+, NH_4^+) and divalent cations (Ca^{2+}, Ba^{2+}, $Sr^{2+}$and Mg^{2+}) was determined to characterise the effects of these ions on sorption for the different tests.

No large differences were observed in the composition of the SGW water after the contact with the Gault or *Plicatules* samples, indicating that no significant dissolution/precipitation effects are expected in the raw clay/synthetic water system. Only a slight increase in bicarbonate content was observed in the water as the S/L increased.

Table 2
Chemical properties of the Synthetic Gault Water (SGW).

Element	($mg \cdot L^{-1}$)
Ba	<0.03
Ca	107 ± 10
Cl	55 ± 3
HCO_3^-	208 ± 10
K	30 ± 6
Mg	46 ± 3
Na	57 ± 5
NH_4^+	<0.1
SO_4^{2-}	430 ± 15
Sr	19 ± 3
pH	7.5 ± 0.2
Conductivity ($\mu S \cdot cm^{-1}$)	1100 ± 50

The same verification was also carried out with the exchanged samples, which were contacted with the respective pure electrolyte. In this case, some ion leaching was observed in the electrolytes at the end of the exchange experiment. In the case of the Na-exchanged system, the presence of divalent ions, especially Ca, which concentration reached values from 2 to $4 \cdot 10^{-4}$ M was particularly relevant since they can act as competing ion. Small quantities of sulphates or carbonates that may affect Ra speciation were also detected.

3.3. Radionuclide and counting techniques

The radionuclide used in this study was ^{226}Ra, supplied by Eckert and Ziegler Isotope Products, as $Ra(NO_3)_2$ in HNO_3 1 M. Ra is supplied with a carrier of Ba (10 $g \cdot mL^{-1}$ solution). ^{226}Ra has a half-life of 1600 years and decays by alpha emission (4.871 MeV) into ^{222}Rn.

The ^{226}Ra decay chain is quite complex and involves numerous daughters; the correct ^{226}Ra measurement requires the equilibrium between all the main daughters (established by the in-growth of shorter lived elements). The in-growth time is 21–23 days (approximately six half-lives of the main ^{226}Ra daughter, ^{222}Rn). Additionally, during this time, samples must be hermetically sealed to avoid Rn escape and ensuring the secular equilibrium between the gas and its progeny (IAEA, 2010).

Liquid Scintillation Counting (LSC) was the technique selected for Ra activity measurements, which provides high efficiency. The alpha-beta counter was a 2700TR liquid scintillation counter and Ultima Gold (Perkin Elmer) was used as scintillation cocktail.

Supporting experiments were also carried out with ^{133}Ba, supplied by Eckert and Ziegler Isotope Products. Ba is in the form of $BaCl_2$ in 0.1 M HCl with a carrier of stable Ba (10 $g \cdot mL^{-1}$ solution). ^{133}Ba has half-life of 10.74 years; it decays by electron capture and presents different gamma emissions from 0.03 to 0.4 MeV. Its activity in solution was measured by γ-counting with a NaI detector (Packard Autogamma COBRA II).

3.4. Sorption tests

Sorption data were obtained using batch sorption techniques. Desorption tests were also carried out to check sorption reversibility. Experiments with the raw samples were carried out in oxygen-free glove box (with N_2 and 1% CO_2), with the clay crushed and sieved (<0.1 μm) suspended in the SGW. The effect of the solid-to-liquid ratio (S/L) and radionuclide concentration was analysed, as well as the kinetics of the sorption process.

Experiments with the exchanged samples were carried out under atmospheric conditions in the respective electrolyte at different ionic strengths; the effects of radionuclide concentration, ionic strength and pH were also analysed.

Sorption kinetics was investigated first to determine the time required to reach the concentration equilibrium. The suspensions traced with the radionuclide were introduced in centrifuge tubes and maintained in continuous stirring during the selected contact time (from 3 to 94 days). After the chosen contact time, the solid and liquid phases were separated by centrifuging (22000×*g*, 30 min), with a JOUAN MR23i centrifuge. After solid separation, three aliquots of the supernatant were extracted from each tube for the analysis of the final Ra activity. The rest of the solution was used to check the final pH.

In sorption experiments, the activity was typically measured in 2 mL of the supernatant, only in the case of very low activity in solution (for example, low tracer concentration in case of high sorption), the volume was increased. Measurements of pH (±0.10) were made using a combined glass pH electrode (Metrohm)

incorporating an Ag/AgCl reference electrode. The electrode calibration was made with buffer solutions at pH 4, 7, and 10.

Sorption isotherms were obtained with the raw samples equilibrated with SGW. In the exchanged samples, sorption isotherms were performed at a fixed pH (approximately between 7 and 7.7) with a fixed background electrolyte concentration. The concentration of radium varied from [Ra] = $5\cdot10^{-10}$ M to [Ra] = $5\cdot10^{-8}$ M, approximately. In the case of Ba, the tracer concentration was extended to approximately $5\cdot10^{-6}$ M in the raw samples and to $1\cdot10^{-3}$ M in the exchanged samples.

Sorption edges (i.e., sorption curves as a function of pH) were obtained with Ra on all the exchanged samples and with Ba on Na-exchanged sample, varying the pH of the suspensions from approximately pH 4 to 10 with 0.1 or 1 M NaOH or HCl; the pH was readjusted, if necessary, after the addition of the radionuclide. The electrolyte (ClO_4^-) concentration in sorption edges was 0.1 M.

The separation and counting procedures for sorption edges and isotherms were the same as that described for kinetics tests.

The degree of sorption observed was represented by the distribution ratio K_d ($mL\cdot g^{-1}$), defined as the ratio of the mass (activity) of the element per unit mass of the solid to the mass (activity) per unit volume of the solution. It is calculated from equation (E.1):

$$K_d = \frac{A_{in} - A_{fin}}{A_{fin}} \cdot \frac{V}{m} \quad (1)$$

where A_{in} and A_{fin} are the initial and final concentrations of the tracer in the liquid phase ($Bq\cdot mL^{-1}$), m the mass of the clay (g) and V the volume of the liquid (mL).

Uncertainty (U) was calculated according to equation (E.2):

$$U(K_d) = \sqrt{\left(K_d + \frac{V}{m}\right)^2 \times \left(\left(\frac{U(A_{in})}{A_{in}}\right)^2 + \left(\frac{U\left(A_{fin}\right)}{A_{fin}}\right)^2\right) + (K_d)^2 \times \left(\frac{U(m/V)}{m/V}\right)^2} \quad (2)$$

Finally, desorption kinetics tests were also carried out using a S/L ratio of 10 $g\cdot L^{-1}$ (Sample 1) using 40 mL of SGW, to provide enough volume to perform several water samplings. Different samples were prepared to get data at different sorption times (1 day, 1 week, 2 weeks, 1 month and 3 months). After the sorption step, where the distribution coefficient was evaluated, all the remaining liquid was discarded and replaced by fresh SGW. The tube with the solid and residual liquid phase was weighted to take into account the contribution of the radionuclide in the residual liquid phase on the calculations. The solid was accurately re-suspended and the sample maintained under continuous agitation. After the selected de-sorption time (1 day, 1 week, 2 weeks, 1 month and 3 months) part of the suspension was sampled and centrifuged to determine the "desorption K_d" ($K_{d(des)}$) (E.3):

$$K_d(des) = \frac{C_{ads,s} - C_{fin,des}}{C_{fin,des}} \cdot \frac{V}{m} \quad (3)$$

where $C_{ads,s}$ is the concentration in the solid after the adsorption step and $C_{fin,des}$ is the concentration of the radionuclide after the desorption steps. The SGW used for these tests was analysed after 5 months in the oxygen-free glove box and the composition was similar to the values reported in Table 2.

3.5. Calculation of selectivity coefficients and complexation constants

Retention of divalent metals onto clays may take place by different mechanisms, such as cation exchange and surface complexation (Tournassat et al., 2013). Considering the sorption behaviour of other divalent alkaline earth element like Ca or Sr in clays, (Missana and García Gutierrez, 2007; Missana et al., 2008), Ra and Ba sorption data will be interpreted considering both retention mechanisms.

The ionic exchange reaction between a cation B, with charge zB, in the aqueous phase; and a cation A, with charge zA, at the clay surface (≡X) can be defined by (E.4):

$$z_B A{\equiv}X + z_A B \Leftrightarrow z_A B{\equiv}X + z_B A \quad (4)$$

The cation exchange reactions can be expressed with selectivity coefficients (E.5; Gaines and Thomas, 1953):

$${}^{B}_{A}K_{SEL} = \frac{(N_B)^{z_A}}{(N_A)^{z_B}} \frac{(a_A)^{z_B}}{(a_B)^{z_A}} \quad (5)$$

where a_A and a_B are the activities of the cations A and B, and N_A and N_B are the equivalent fractional occupancies. Selectivity coefficients of a cation, at trace concentrations, can be determined by sorption measurements (Bradbury and Baeyens, 1994). If the cation B is present at trace levels, then N_A (E.5) is approximately 1; furthermore, if the distribution coefficient of the exchange process (K_d) is known, then the selectivity coefficient can be determined with the following relation (E.6):

$${}^{B}_{A}K_{SEL} = \left(\frac{K_d \cdot z_B}{CEC}\right)^{z_A} \frac{\gamma_A^{z_B}}{\gamma_B^{z_A}} (A)^{z_B} \quad (6)$$

where γ_A and γ_B are the solution activity coefficients of cations A and B. Cation exchange capacity (CEC) used in the calculations corresponds to the mean value of the measurements obtained in present work for the exchanged clays, that is 14.7 $meq\cdot 100\ g^{-1}$.

The activity coefficients (γ) at 20 °C, can be calculated with the Davies approximation (E.7):

$$Log\gamma_i = -0.51\cdot z_i^2 \left(\frac{\sqrt{I}}{1+\sqrt{I}} - 0.3\cdot I\right) \quad (7)$$

where I represents the ionic strength of the solution.

For experiments with Na-exchanged or NH_4-exchanged samples, E.6 becomes:

$${}^{Ra}_{Na}K_{SEL} = \left(\frac{K_d x\ 2}{CEC}\right) \frac{\gamma_{Na}^2}{\gamma_{Ra}} (Na)^2 \quad (8a)$$

and

$$ {}^{Ra}_{NH_4}K_{SEL} = \left(\frac{K_d \ x \ 2}{CEC}\right) \frac{\gamma^2_{NH4}}{\gamma_{Ra}}(NH_4)^2 \quad (8b) $$

For experiments with Ca-exchanged and Ba-exchanged samples, E.6 is:

$$ {}^{Ra}_{Ca}K_{SEL} = \left(\frac{K_d}{CEC}\right)^2 \frac{\gamma^2_{Ca}}{\gamma^2_{Ra}}(Ca)^2 \quad (8c) $$

$$ {}^{Ra}_{Ba}K_{SEL} = \left(\frac{K_d}{CEC}\right)^2 \frac{\gamma^2_{Ba}}{\gamma^2_{Ra}}(Ba)^2 \quad (8d) $$

These analytical expressions are valid for a simple cation exchange process at a single site, and allow the determination of selectivity coefficients directly from the sorption curves in the region where this process is dominant. However, the parameters might be biased either by the presence of other ions competing for the sorption site, by the presence of multiple sorption sites or the occurrence of sorption mechanisms other than ion exchange (Missana et al., 2014). For this reason, when calculated from the experimental data, the selectivity coefficients will be referred to as "apparent". These (apparent) selectivity coefficients were calculated for each set of data with the exchanged samples.

For ionic exchange processes, sorption is assumed to be independent on pH and the theoretical dependence on electrolyte concentration, A, derived from the previous equations is the following (E.9):

$$ z_A \cdot Log(K_d) = -z_B Log(A) + Log\left(\frac{{}^{B}_{A}K_{SEL}(CEC)^{z_A}\gamma_B^{z_A}}{z_B^{z_A}\gamma_A^{z_B}}\right) \quad (9) $$

Thus, for a homovalent exchange (Ra-Ca or Ra-Ba), the dependence of Log(K_d) on Log(A) is represented by a line with a slope of −1. For heterovalent exchange (Ra-Na or Ra-NH_4) the theoretical dependence is a line with slope of −2.

As the theoretical dependence of sorption for a simple ion exchange mechanism was not always satisfied, the model assumes that, in the experiments in Na-exchanged and NH_4-exchanged samples at high ionic strength values, Ra sorption in High Energy Sites (HES) contributes to the overall Ra retention in a non-negligible way. This reaction is assumed to be a Me-Mg substitution on the edge termination of an octahedral sheet of the clay, as described in Tournassat et al. (2013). The corresponding reaction on the HES sites is described in E.10 in a simplified way:

$$ S_{HES}Mg + Ra^{2+} \Leftrightarrow S_{HES}Ra + Mg^{2+} \qquad K_{HES} \quad (10) $$

If surface complexation on amphoteric sites (SOH) existing in the clay is considered, the protonation/deprotonation reactions of the SOH are (E.11 and E12):

$$ SOH_2^+ \Leftrightarrow SOH + H^+ \qquad K^+ \quad (11) $$

$$ SOH \Leftrightarrow SO^- + H^+ \qquad K^- \quad (12) $$

where SOH_2^+, SOH and SO^- represent the positively charged, neutral and negatively charged surface sites, respectively. K^+ and K^- are the intrinsic equilibrium acidity constants.

Ra adsorption onto SOH sites can be described with reactions of this type (inner sphere complexation; E.13):

$$ SOH + Ra^{2+} \Leftrightarrow SORa^+ + H^+ \qquad K_c \quad (13) $$

The verification of the experimentally determined parameters, in addition to other modelling calculations on the effects of multiple sites and/or competing ions on sorption, were performed with the CHESS v 2.4 code (Van der Lee and De Windt, 1999) and with the PhreeqC code vs 3.3 (Parkhurst and Appelo, 2013) using ThermoChimie database version 9 (Giffaut et al., 2014). The fit of the experimental curves was obtained with a trial and error procedure.

4. Results

4.1. Cation exchange capacity (CEC) and surface reactive area

CEC measurements on Sample 1 and the different exchanged samples were performed using the copper(II) ion complex with trietylenetetramine $[Cu(trien)]^{2+}$ as index cation and BET specific surface was determined by N_2 adsorption. The Sample 1 CEC was 14.0 ± 0.1 meq·100 g^{-1} and the N_2-BET = 24.4 ± 0.2 $m^2 \cdot g^{-1}$. No significant differences in CEC or BET were detected for any of the exchanged samples, which presented, in average, slightly higher values than the raw sample (CEC 14.7 ± 0.4 meq·100 g^{-1} and BET 26.9 ± 1.9 $m^2 \cdot g^{-1}$). The CEC of the other samples varied from 8.6 to 15 meq·100 g^{-1}.

4.2. Tests with raw clay samples

The dependence of Ra sorption on time and on the solid-to-liquid ratio was studied first. The sorption kinetics (from 1 h to 92 days) of Ra on Sample 1 and synthetic Gault water (SGW) shows small kinetic effects as K_d values tend to increase with time from approximately logK_d = 2.15 to 2.65 (Fig. 1a). The main increase in sorption is observed within the first week and then equilibrium is attained; the standard contact time for additional experiments was established at 10 days.

Concerning the sorption dependence on S/L, the K_d values measured on Sample 1 tend to decrease rapidly when the solid to liquid ratio increases, thus the largest variation is observed from 1 to 10 g·L^{-1} (with logK_d from 2.7 to 2.1) (Fig. 1b). Similar trend is observed for Sample 8. For further tests the standard S/L ratio selected was 10 g·L^{-1}, because K_d values obtained with this S/L are very near to the "saturation" value.

The effect of the radionuclide concentration on sorption was studied on five raw samples (Samples 1, 3, 8, 9 and 15 in Table 1) equilibrated with SGW. The initial concentration of Ra ranged from approximately $5 \cdot 10^{-10}$ to $5 \cdot 10^{-8}$ M, and the radioactivity of ^{226}Ra hampered the use of this radionuclide at higher concentration. Sorption of Ba was studied for a wider range of concentrations, up to $5 \cdot 10^{-6}$ M, in SGW. Main results are summarized in Table 3. The adsorption of both alkaline earth ions is relatively constant in the range of concentrations analysed (Fig. 2a and b). A decrease of the K_d values at high concentrations was not observed, which seems to indicate that sorption sites are not saturated under those experimental conditions.

For the last point of Ba isotherm ([Ba] ~ $5 \cdot 10^{-6}$ M), precipitation of barite ($BaSO_4$) is suspected. Speciation calculations show that, under those conditions, the aqueous barium sulphate complex is formed, and calculated barite ($BaSO_4$) saturation index is above 0. Also for Ra, precipitation (in the form of (Ba,Ra)SO_4 solid solution) cannot be excluded at the higher tracer concentrations used in the experiments, as barium (used as a carrier in Ra radiotracer solution) is also present in the samples. On the other hand, saturation of sorption sites (e.g., a decrease of K_d values at high concentrations) was not detected in these isotherms.

4.3. Desorption tests

Desorption kinetics tests with Ra were carried out on Sample 1

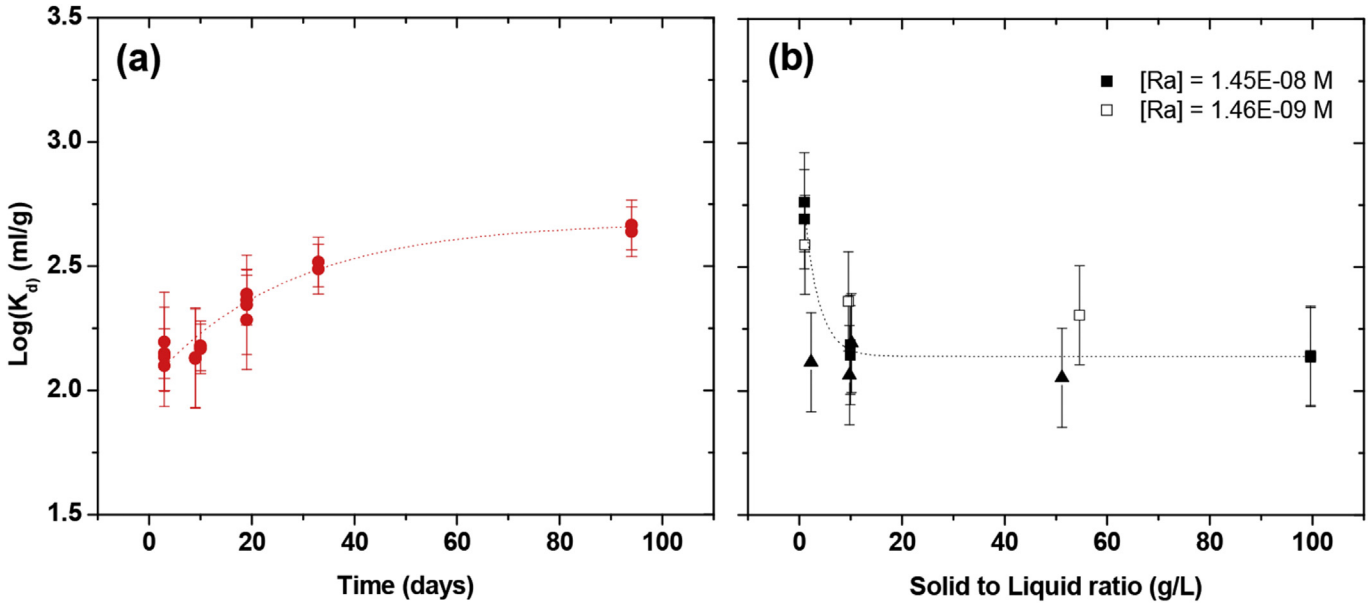

Fig. 1. a) Sorption kinetics of Ra in Sample 1 (10 g·L^{-1}). [Ra] = 1.8·10^{-8} M; b) Sorption dependence of Ra with the S/L ratio on Sample 1 (circles) and Sample 8 (triangles). Full points refer to [Ra] = 1.45·10^{-8} M and open points to [Ra] = 1.45·10^{-9} M.

Table 3
K_d mean values (mL·g^{-1}) obtained on the different raw samples from the sorption isotherms.

Sample	Ra (mL·g^{-1})	Ba (mL·g^{-1})
Sample 1	169.1 ± 22.1	74.2 ± 4.2
Sample 3	251.9 ± 19.8	59.8 ± 1.6
Sample 8	179.2 ± 21.2	35.1 ± 1.5
Sample 9	299.7 ± 22.1	71.6 ± 8.5
Sample 15	825.3 ± 57.9	269.1 ± 11.6

(10 g·L^{-1}). At shorter times, desorption K_d's are always slightly higher than sorption K_d's. This might indicate incomplete reversible sorption; at longer times all K_d's tend to be very similar and comparable to sorption values (Fig. 3). These results basically show that, if enough time is given to reach the equilibrium, Ra sorption in this system is reversible, even if kinetic effects are observed both in sorption and in desorption steps.

4.4. Tests with the exchanged clays

A number of experiments were carried out with Gault exchanged clays, prepared from Sample 1, to better understand Ra sorption behaviour and to determine parameters useful for sorption modelling (selectivity coefficients and/or complexation constants). The study with exchanged clays aimed to analyse the effects of electrolyte concentration, main exchanging cations, pH and Ra concentration on the four Gault exchanged samples (Na-exchanged, NH_4- exchanged, Ca-exchanged and Ba-exchanged). The summary of all experiments performed with Ra and results is given in Table 4. Supporting tests with Ba in Na- and Ca-exchanged samples were also carried out.

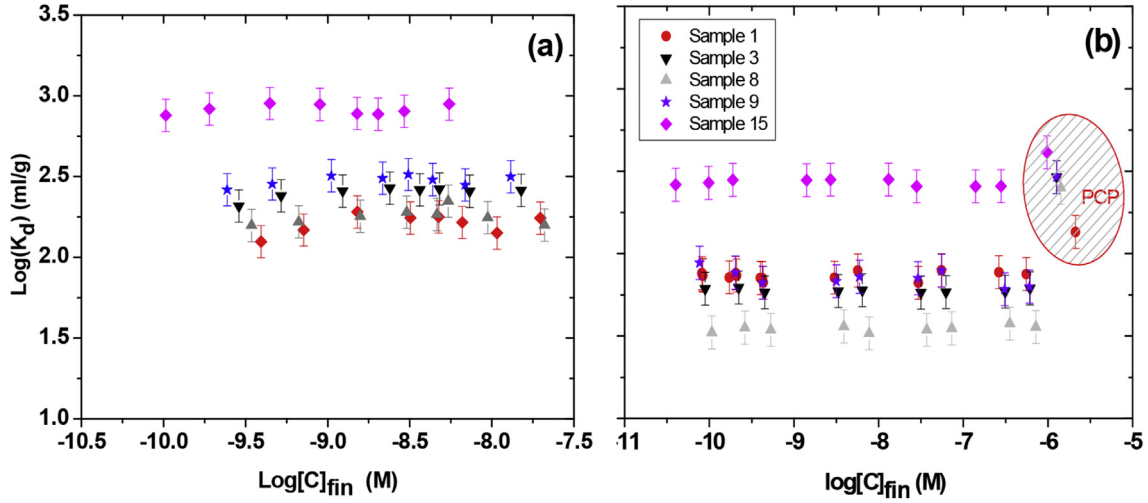

Fig. 2. Sorption isotherms of (a) radium and (b) barium on the raw samples, described in Table 1, suspended in SGW. "PCP"-shaded area indicates the data suspected to be affected by barite precipitation.

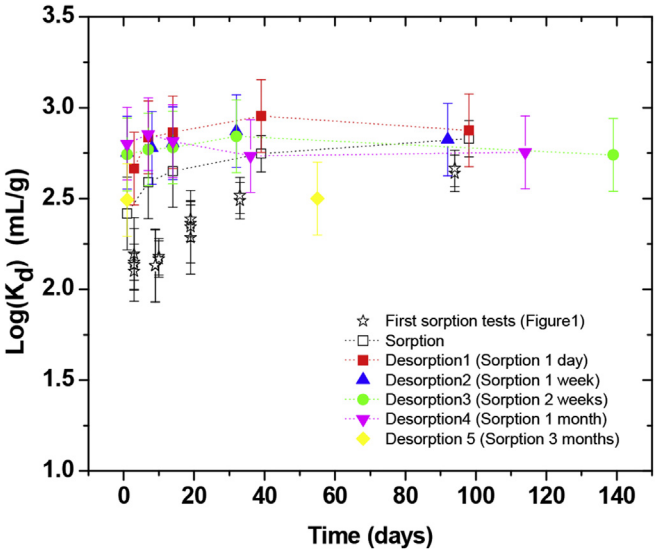

Fig. 3. Desorption of radium from the Sample 1 through time.

In all the cases, sorption increases with pH suggesting the existence of Ra surface complexation with amphoteric surface functional groups (Fig. 4). Most of the data are obtained at pH > 7 because pH was difficult to maintain stable at lower values (from 4 to 7) even with buffers. Consequently, the determination of the selectivity coefficients for ionic exchange process in a region where exchange is little affected (or not affected at all) by surface complexation is less accurate. Thus, the "apparent" selectivity coefficient determined from experimental data might be slightly overestimated.

The sorption isotherms and the dependence of the logK$_d$ on the logarithm of electrolyte concentration (E.9) carried out with Ra with the four exchanged samples are shown in Figs. 5 and 6, respectively. For each experimental condition, radium adsorption is relatively constant in the range of concentrations studied. At high electrolyte concentration, radium adsorption on NH_4- exchanged sample is lower than that observed on Na-exchanged sample whereas the opposite is true at low concentration. Similarly, the significantly lower Ra adsorption in Ba-exchanged sample indicates that Ba is a much stronger competing divalent ion for Ra than Ca.

Additional supporting experiments were carried out with Ba on Na- and Ca-exchanged samples. In particular, sorption dependence on pH, ionic strength and tracer concentration was analysed. Fig. 7 shows Ba sorption edges (at two different Ba concentrations) in 0.1 M $NaClO_4$. The dependence on pH in Na-Gault seems less pronounced in the case of Ba than that observed for Ra.

The sorption isotherm with Ba (Fig. 8) is carried out in a wider range of concentrations than that of Ra. Ba sorption is linear over approximately four orders of magnitude (up to $1\cdot10^{-6}$ M approximately), then sorption sites are progressively saturated leading to a K$_d$ decrease with increasing Ba concentration. Even at very high Ba concentration (10^{-3} M) precipitation of Ba salts is not observed (contrary to the case of raw samples) since sulphate content in the electrolyte is lower. As for radium, sorption clearly decreases as the ionic strength increases.

5. Discussion and modelling

5.1. Raw clays

The increase in sorption with time observed within the first week of experiments agrees with the fact that sorption processes (especially ionic exchange) are usually fast. The further slower and

Table 4
Summary of Ra sorption results obtained with the exchanged samples. Contact time 10 days. S/L 10 g·L^{-1}. The logarithm of the apparent selectivity coefficient determined from sorption tests is also indicated.

Test type	Sample	Electrolyte and Conc.	pH	[Ra] (M)	LogK$_d$ (mL·g^{-1})
Isotherm	Na-exchanged	$NaClO_4$ 0.1 M	7.67 ± 0.13	$4.2\cdot10^{-10}$ to $1.2\cdot10^{-8}$	2.55 ± 0.09
Isotherm	Na-exchanged	$NaClO_4$ 0.01 M	7.73 ± 0.05	$4.2\cdot10^{-10}$ to $1.2\cdot10^{-8}$	3.22 ± 0.05
Isotherm	Na-exchanged	$NaClO_4$ 0.3 M	7.51 ± 0.06	$4.2\cdot10^{-10}$ to $1.2\cdot10^{-8}$	2.14 ± 0.02
Edge	Na-exchanged	$NaClO_4$ 0.1 M	variable	$4.2\cdot10^{-9}$	2.09 to 3.50
Isotherm	NH_4-exchanged	NH_4ClO_4 0.1 M	7.47 ± 0.02	$8.2\cdot10^{-10}$ to $2.4\cdot10^{-8}$	1.72 ± 0.05
Isotherm	NH_4-exchanged	NH_4ClO_4 0.1 M	7.00 ± 0.02	$4.2\cdot10^{-9}$ to $8.3\cdot10^{-9}$	1.64 ± 0.05
Isotherm	NH_4-exchanged	NH_4ClO_4 0.01 M	7.56 ± 0.05	$8.2\cdot10^{-10}$ to $2.4\cdot10^{-8}$	3.53 ± 0.06
Edge	NH_4-exchanged	NH_4ClO_4 0.1 M	7.47 ± 0.07	$4.1\cdot10^{-9}$	1.56 to 1.94
Isotherm	Ca-exchanged	$Ca(ClO_4)_2$ 0.033 M	7.47 ± 0.15	$1.5\cdot10^{-10}$ to $4.5\cdot10^{-9}$	2.43 ± 0.04
Isotherm	Ca-exchanged	$Ca(ClO_4)_2$ 0.003 M	7.51 ± 0.06	$1.5\cdot10^{-10}$ to $4.5\cdot10^{-9}$	3.25 ± 0.02
Isotherm	Ca-exchanged	$Ca(ClO_4)_2$ 0.1 M	7.23 ± 0.06	$4.9\cdot10^{-9}$ to $1.2\cdot10^{-8}$	2.06 ± 0.01
Edge	Ca-exchanged	$Ca(ClO_4)_2$ 0.033 M	variable	$1.0\cdot10^{-8}$ to $9.8\cdot10^{-7}$	2.22 to 2.89
Isotherm	Ba-exchanged	$Ba(ClO_4)_2$0.033 M	7.01 ± 0.04	$8.2\cdot10^{-10}$ to$2.4\cdot10^{-8}$	0.66 ± 0.23
Isotherm	Ba-exchanged	$Ba(ClO_4)_2$ 0.003 M	7.16 ± 0.04	$8.2\cdot10^{-10}$ to $2.4\cdot10^{-8}$	1.64 ± 0.02
Edge	Ba-exchanged	$Ba(ClO_4)_2$ 0.033 M	variable	$1.0\cdot10^{-8}$ to $9.8\cdot10^{-7}$	0.60 to 1.2

Table 5
Parameters used for the modelling of Ra and Ba sorption in exchanged samples.

Parameter	Value		Reference
CEC (mean)	5.46 μeq·m^{-2}		This work
SOH density	0.95 μeq·m^{-2}		Missana et al. (2009)
S_{HES} density	2.5 mmol kg^{-1}		Tournassat et al. (2013)
Reactions and LogK			
SO[-] composition = −1 H[$^{+}$], 1 SOH	logK = −9.5		Missana et al. (2009)
SOH_2[+] Composition = 1 H[$^{+}$], 1 SOH	logK = 4.5		Missana et al. (2009)
Gault-Ra[+] (surface complexation) composition = 1 SOH, −1 H[$^{+}$], 1 Ra[$^{2+}$]	logK = −4.6		This work
Gault-Ba[+] (surface complexation) composition = 1 SOH, −1 H[$^{+}$], 1 Ba[$^{2+}$]	logK = −6.0		This work
S_{HES}-Ra composition = 1 S_{HES}Mg, −1 Mg[$^{2+}$], 1 Ra[$^{2+}$]	logK = 2.1		This work
S_{HES}-Ba composition = 1 S_{HES}Mg, −1 Mg[$^{2+}$], 1 Ba[$^{2+}$]	logK = 1.8		This work
	Ra	**Ba**	
Na-Gault			
Gault(Ra/Ba) (exchange) composition = 2 Gault(Na), −2 Na[$^{+}$], 1 Ra/Ba[$^{2+}$]	logK = 0.44 (low I)	logK = −0.58 (low I)	This work
NH_4-Gault			
Gault(Ra) (exchange) composition = 2 Gault(NH_4), −2 NH_4[$^{+}$], 1 Ra[$^{2+}$]	logK = 0.75 (low I)	Nd	This work
Ca-Gault			
Gault(Ra/Ba) (exchange) composition = Gault(Ca), −1 Ca[$^{2+}$], 1 Ra/Ba[$^{2+}$]	logK = 2.05	logK = 1.33	This work
Ba-Gault			
Gault(Ra) (exchange) composition = Gault(Ba), −1 Ba[$^{2+}$], 1 Ra[$^{2+}$]	logK = 0.28	nd	This work

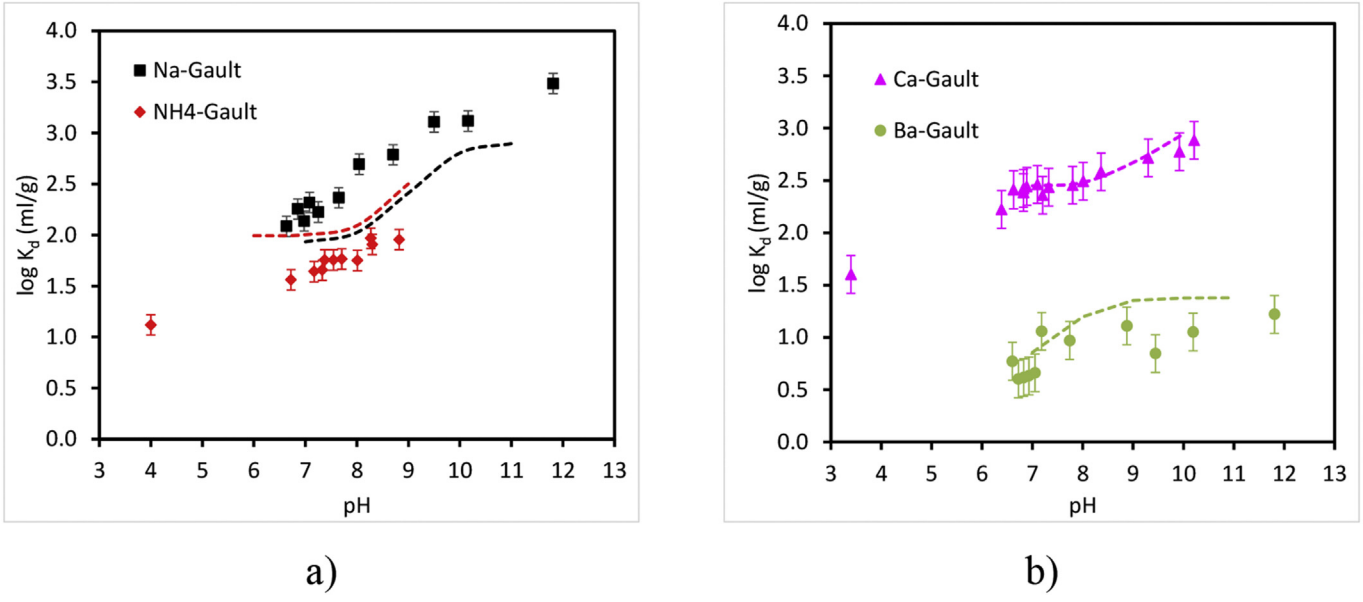

Fig. 4. Radium sorption edges on a) Na-exchanged and NH_4-exchanged samples in 0.1 M $NaClO_4$/NH_4ClO_4; b) Ca-exchanged and Ba-exchanged samples in 0.03 M $Ca(ClO_4)_2$/$Ba(ClO_4)_2$. [Ra] = 4.1·10^{-9} M. Dashed lines represent the fit of the data with the parameters of Table 5.

small increase in sorption might be caused by processes other than sorption, as diffusion or incorporation of radium in minerals present in the solid (for example within calcite). Slow precipitation of sulphates (Ra-barite) or carbonates cannot be also ruled out. In particular, the interaction of Ba and Ra with carbonate minerals has been reported in the literature (Shahwan et al., 2002; Ghaemi et al., 2011; Jones et al., 2011; Tunusoglu et al., 2007). Shahwan et al. (2002) observed that in bentonite clay, the presence of $CaCO_3$ increased the retention of Ba, probably due to the formation of $BaCO_3$ (witherite); this occurred particularly at high pH and low Ba^{2+} concentrations. Also Tunusoglu et al. (2007) observed that $BaCO_3$ precipitation enhanced the uptake of barium in calcite and aragonite and reported that witherite was formed in a kinetically slower process than sorption. Jones et al. (2011) observed two types of reactions predominating retention of Ba/Ra in different minerals; in siderite, ankerite or magnesite sorption appeared to be the main

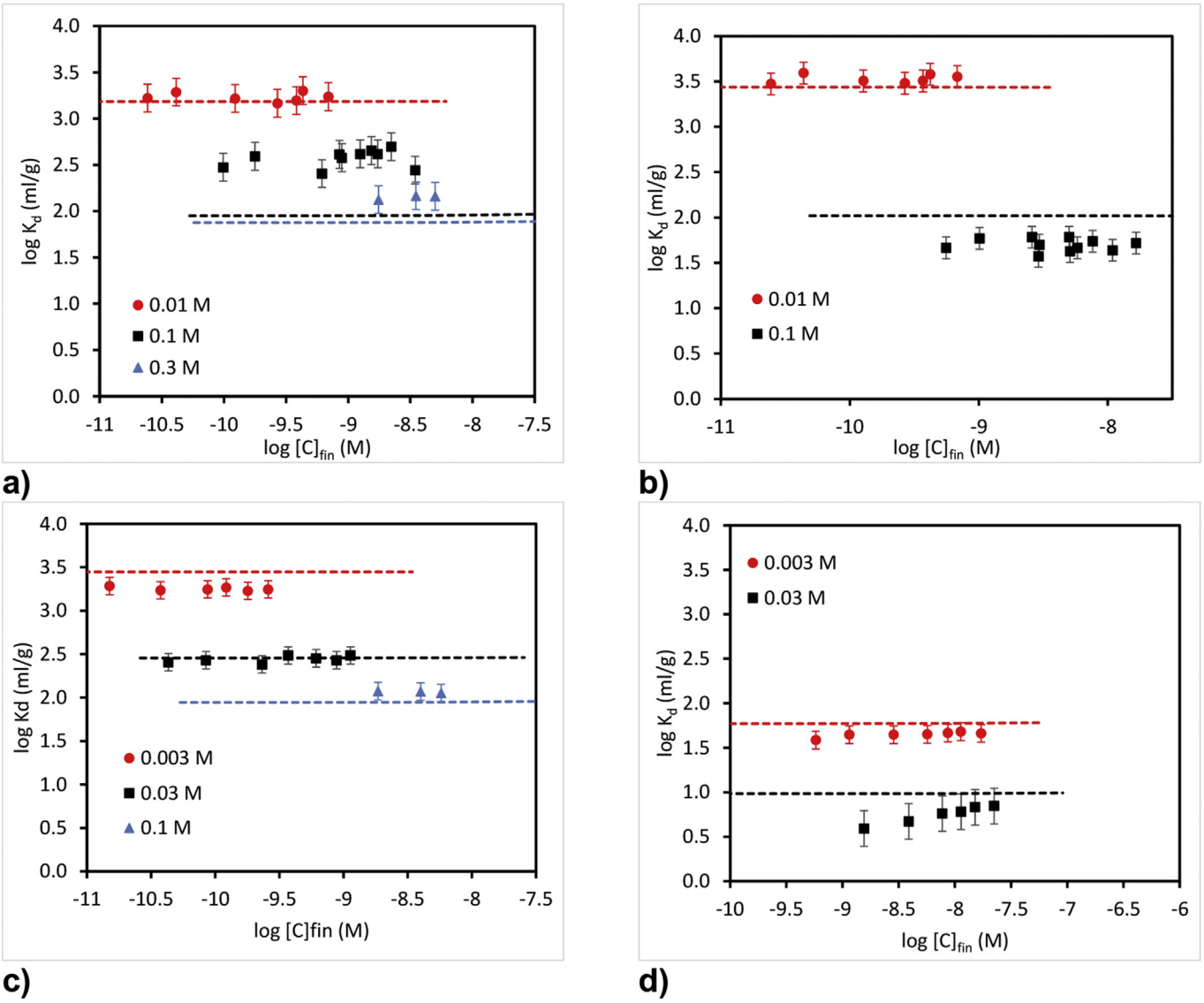

Fig. 5. Sorption isotherms of Ra on (a) Na-exchanged; (b) NH_4-exchanged; (c) Ca-exchanged and (d) Ba-exchanged samples in the respective electrolytes at different concentrations. Dashed lines represent the fit of the data with the parameters of Table 5.

mechanism of Ra incorporation, whereas in others like calcite, dolomite and strontianite, the main retention mechanism was co-precipitation.

The decrease of sorption with increasing mass of solid does not seem to be related to the presence of soluble salts in the clay. At lower S-L ratio, the amount of dissolved competing ions would be lower, inducing less competitive effects and, therefore, higher K_d values. However, this hypothesis is not supported by the analyses of the chemical composition of the water in contact with the raw clay. In fact, the chemical composition of the SGW contacted with different quantity of solid was very similar.

Other authors observed similar dependence of Ba and Ra sorption on the S/L (higher S/L the lower K_d until a "asymptotically" minimum value is reached) (Tamamura et al., 2014; Görtürk et al., 1995; Erten and Gokmenoglu, 1994; Eylem et al., 1990; Meier et al., 1987). The observed effect could be mainly related to the kinetic effects in sorption. In more diluted, better dispersed suspensions the tracer may reach faster all the available sorption sites whereas in the more concentrated ones the process may be slower.

All the samples, except Sample 15, showed similar K_d values, from 170 to 300 $g \cdot mL^{-1}$ for Ra and from 30 to 70 $g \cdot mL^{-1}$ for Ba; sample 15 shows the highest sorption capability for both elements (3–4 times higher). The difference in the mineralogy of this sample does not clearly explain the higher K_d values observed in sample 15. The main difference observed in FTIR analyses for Sample 15 with respect to Sample 1 and 8 is the presence of a Fe-rich mineral with a tri-octahedral character (iron–rich smectite). There is also no clear difference between sample 8 and the others (except sample 15) indicating a relatively similar behaviour between Gault Fm and *Plicatules* Fm.

Barium and radium are frequently considered as analogues. However, sorption values obtained for Ra are a half an order of magnitude higher than that measured for Ba (Fig. 2 and Table 3). These results indicate the higher selectivity of Ra with respect Ba in the studied clays. In fact, the sorption behaviour of metal ions with the same charge is expected to depend on their ionic radium and hydration energies. If the ionic radium is large, the charge density of the ion is small and lower hydration is expected. Then, under the same experimental conditions, higher adsorption is expected for Ra, that has a larger ionic radium (Ra = 1.43 Å), than for barium

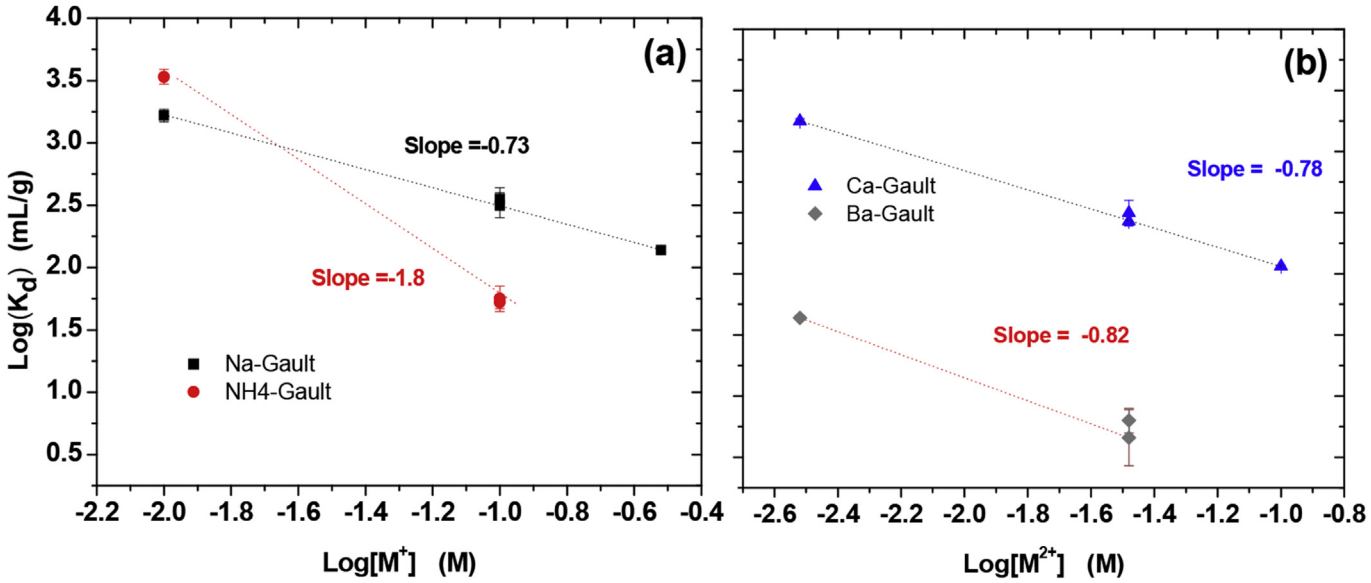

Fig. 6. Dependence of Log K_d on the electrolyte concentration (E.6) (see section 5.2 for the discussion of this dependence). (a) Monovalent electrolytes; (b) Divalent electrolytes.

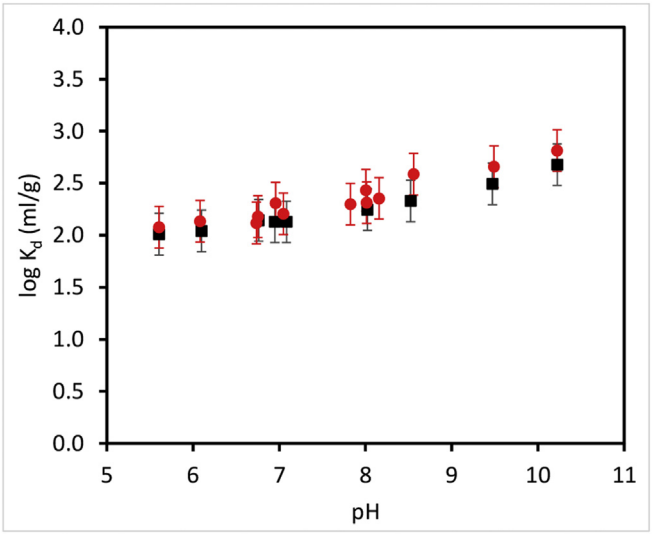

Fig. 7. Sorption edges on Na-exchanged sample in 0.1 M $NaClO_4$ at two Ba concentrations (●) [Ba] = $3.5 \cdot 10^{-10}$ M and (■) [Ba] = $9.7 \cdot 10^{-7}$ M.

(Ba = 1.34 Å). Following the same reasoning, Sr, which has an even smaller ionic radium, would be even a worse analogue for Ra.

5.2. Exchanged clays

K_d 's obtained for Ba in the Ca-Gault exchanged sample (Fig. 9a) are lower than that measured for Ra (Fig. 5b). Considering that the main exchangeable ions in the raw samples are Ca and Mg, this agrees with the lower K_d values measured for Ba than Ra in the raw materials.

Ra sorption on exchanged clay samples depends on the ionic strength and increases as the ionic strength decreases (Fig. 6). As already mentioned, in a ionic exchange process, for a 2:1 exchange (Ra/M^+, where M^+ is Na or NH_4) the dependence of the logK_d with the electrolyte concentration should be linear with a slope of −2 (E.9). For a 2:2 exchange (Ra/M^{2+}, where M^{2+} is Ca or Ba) the dependence of the logK_d with electrolyte concentration should be linear with a slope of −1 (E.9). In the case of Ra adsorption in the Na-exchanged sample (Fig. 6a), the slope measured (−0.7) is much lower than expected, indicating that other processes than ionic exchange in the clay might be involved in Ra retention. In the case of NH_4 −exchanged sample the slope of the linear fit is −1.8 (Fig. 6a), although only two ionic strengths were tested.

A similar situation is observed in the case of Ba, for which the dependence of Ba sorption on ionic strength neither agrees with a pure ionic exchange process. LogK_d data from the isotherms and from other tests of Ba sorption obtained at different ionic strengths show their dependence on the logarithm of the Na concentration (Fig. 8b).

The deviation from the theoretical dependence on ionic strength is often attributed to the presence of ions leached from the clays into the electrolyte (Missana et al., 2014). In this case, divalent ions were found in concentrations up to $4 \cdot 10^{-4}$ M (Ca); however, sensitivity test calculations performed in order to verify this hypothesis did not provide satisfactory results.

Tamamura et al. (2014) studied the effects of electrolyte concentration on ^{226}Ra adsorption onto Na-exchanged montmorillonite and kaolinite. In both minerals, the dependence of adsorption on the electrolyte concentration was observed. However, the expected dependence for a 1:2 exchange was not observed. Atun and Bascetin (2003) studied the effects of ionic strength on barium sorption on kaolinite, illite and montmorillonite. They observed an increasing sorption with decreasing ionic strength and fitted the data with Freundlich isotherms. However, from their analyses they suggested that "the number of total adsorption sites at high ionic strength is higher than at lower ionic strength" which does not seem to be consistent with a simple ionic exchange concept, and the observation is in agreement with results observed in the present study. Zhang et al. (2001) studied by EXAFS the structure of Ba surface complexes with exchanged Na-montmorillonite as a function of pH and electrolyte concentration. They observed a slight increase of Ba sorption with increasing pH but a more significant increase when the electrolyte concentration in solution decreased. They suggested that most Ba is adsorbed as outer sphere complex in the basal surfaces but that inner-sphere surface complexes are always present at a small concentration, even at acidic pH (4.3). The analysis of sorption data

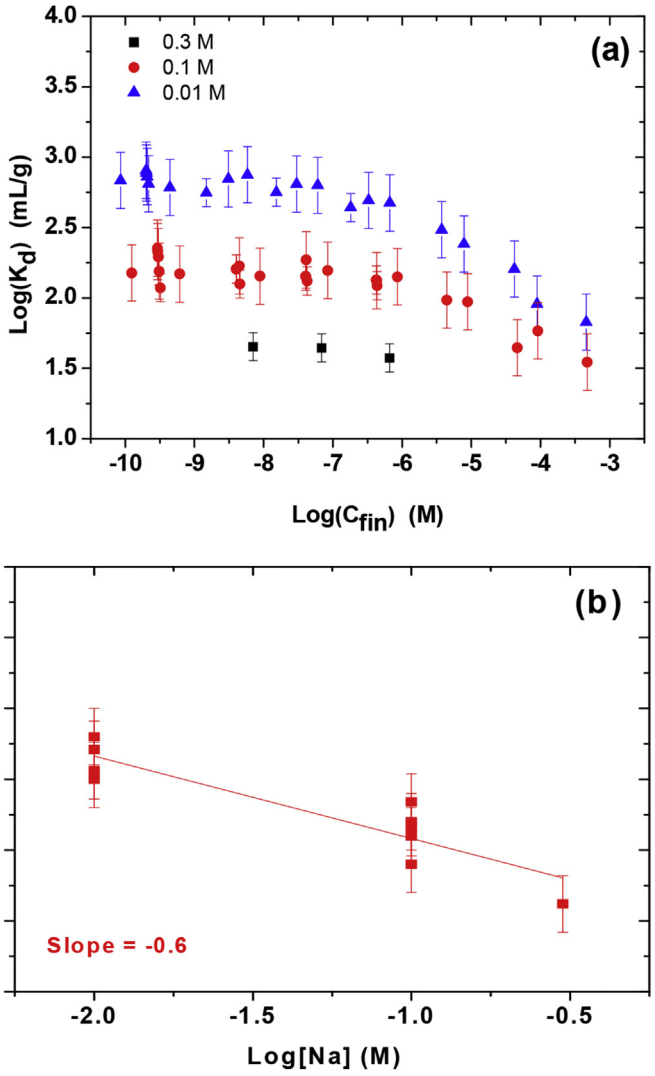

Fig. 8. a) Ba sorption isotherms on the Na-exchanged sample (pH 7.2 ± 0.4) at three different ionic strengths (▲) 0.01 M; (●) 0.1 M and (■) 0.3 M $NaClO_4$. b) Dependence of Log K_d on the electrolyte concentration (E.6) (see section 5.2 for the discussion of this dependence).

dependence on ionic strength from Zhang et al. (2001) showed that it does not fit to the theoretical dependence expected for ionic exchange similarly to our case.

In the case of Ca- and Ba-exchanged samples, the dependence of sorption on the ionic strength (Fig. 6b) presented a slope of approximately −0.8, not dramatically different from the expected theoretically for ionic exchange (−1). The relatively small difference could be explained by the presence of competing ions in solution. For comparison, Ba sorption in Ca-exchanged samples clay also shows a linear dependence on the ionic strength with a slope of −0.92 (see Fig. 9b below), which agrees with that expected for cationic exchange.

The sorption edge and isotherm data suggest that more than one mechanism is involved in Ra and Ba sorption on Gault formation. In order to handle that, we have included Ra sorption in High Energy Sites (HES) as a retention mechanism; this retention has been represented as a Me-Mg substitution, in agreement with the suggestions in Tournassat et al. (2013).

The dependence on pH shows that inner sphere complexes must exist. The increase of Ba adsorption at higher pH is interpreted by Zhang et al. (2001) as the formation of inner sphere complexes considering the sharing of oxygen atoms from deprotonated SOH groups in octahedral layer, i.e., surface complexation. However, the visibility (by EXAFS) of inner sphere complexation also in the region were Ba adsorption is insensitive to pH and may indicate the existence of other types of inner sphere complexes than those with deprotonated SOH. The point is if these complexes can be related to the surface complexation with SOH, whose density is limited (in the order of mmol·L^{-1}) and then maybe not perfectly distinguishable by EXAFS. The quantitative measurements of inner sphere complexes supposedly located at the edges of montmorillonite could have not been performed in Zhang et al. (2001).

5.3. Modelling

The first step was to obtain the selectivity coefficients for ion exchange using the experimental data from exchanged samples. These values were used as initial parameter in the modelling and then were adjusted considering also the results of the sorption edges. The presence of Ba as carrier in Ra radiotracer solution has been taken into account in data modelling.

A single selectivity coefficient cannot reproduce sorption data of Ra in Na-exchanged or NH_4- exchanged samples (Fig. 5a and b), or sorption data of Ba in Na-exchanged samples (Fig. 8a), due to the dependence on ionic strength (Figs. 6a and 8b). In those cases, cation exchange has been assumed to be responsible for radium sorption only at low ionic strength. In the experiments in Na-exchanged and NH_4- exchanged samples at high ionic strength values, Ra or Ba sorption in HES sites has been included in the model.

The pH-dependence of Ra sorption in both Ca- and Ba-exchanged samples is small but not negligible (Fig. 4). Thus, the fitting of sorption edges in exchanged samples, considering both ionic exchange and surface complexation, was performed. The fit of the sorption edges was done adjusting the experimental (apparent) selectivity coefficient to the data obtained at the lower pH, were ion exchange must predominate, and adjusting the logK_c from E.12 (surface complexation constant). The pKs of protonation/deprotonation of the SOH sites and their density were considered to be the same as those of the Illite du Puy, used in previous studies (Missana et al., 2009). The values used for the fit of all the experimental data are summarized in Table 5 and the simulation included as dashed lines on the experimental points in the different figures (edges, Fig. 4, and isotherms, Fig. 5).

Ra sorption data (including the isotherms) in all the exchanged samples are fit reasonably well. The possible effect of other ions present in solution other than Na and ClO_4^-, for example sulphates or carbonates have not been taken into account.

6. Conclusions

The retention capacity of radium in clay rocks is a fundamental aspect in the performance assessment of Ra-bearing waste repository. This article was intended to broaden the existing knowledge of radium sorption in clay rocks using samples from geological formations that are studied as potential host rock formation for a Ra-bearing waste repository in France. In particular, the kinetics and reversibility of the sorption processes, the effects of solid-to-liquid ratio and radionuclide concentration on Ra uptake were investigated on raw samples. To better understand and model the mechanisms of Ra retention on these natural clayey systems, additional tests were carried out with the samples exchanged with four different cations (Na, NH_4, Ca and Ba). The experiments with NH_4 are of special interest since NH_4NO_3 is one of the main waste components and it is expected that this ion would compete with Ra

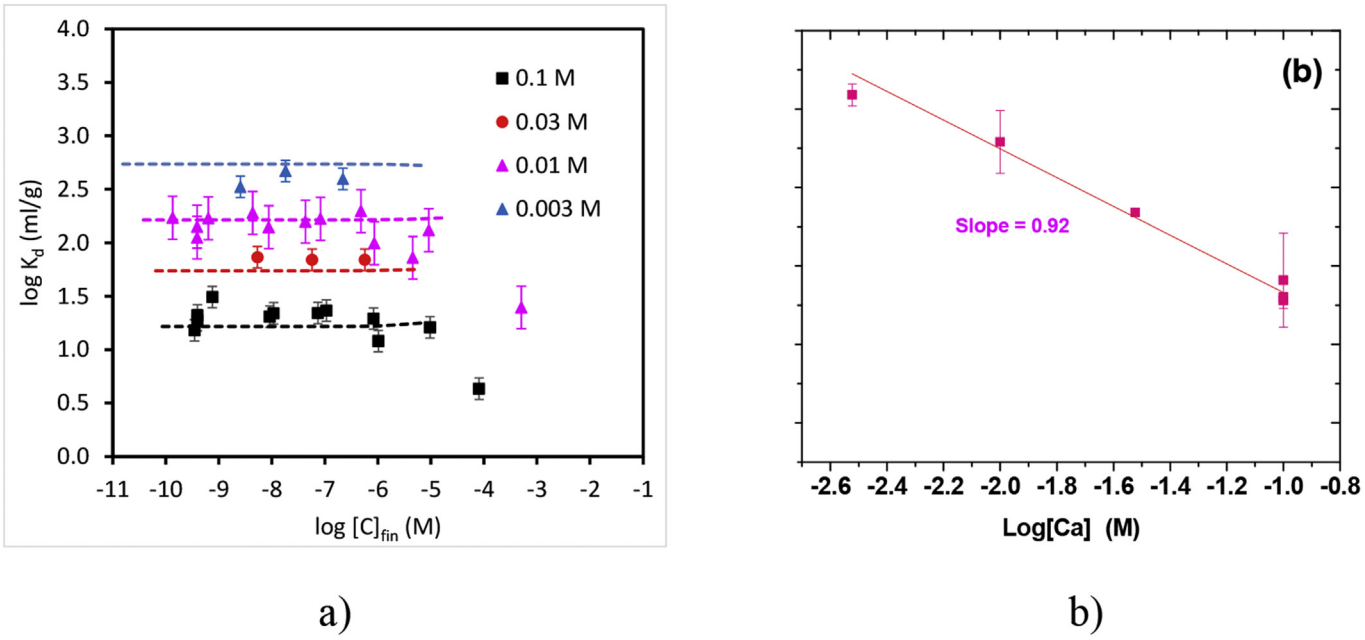

Fig. 9. a) Ba Sorption isotherms on Ca-exchanged sample: (a) 1 $g \cdot L^{-1}$ at two different [Ca] concentrations; (b) 10 $g \cdot L^{-1}$ at three different [Ca] concentrations b) Dependence of Log K_d on Ca-exchanged sample on the electrolyte concentration (E.6).

for sorption sites.

Results indicate that Ra sorption in the raw samples is linear (within the range of concentration investigated) and higher than Ba sorption in the same samples. The presence of carbonates and sulphate may affect the retention in the system and most probably the kinetic of retention processes. In most of the samples, K_d values from 170 to 300 $g \cdot mL^{-1}$ were measured for Ra and from 30 to 70 $g \cdot mL^{-1}$ for Ba. The analogy between Ba and Ra sorption often mentioned in literature is clearly not evidenced in this study demonstrating the need to work with radium to quantify retention appropriately.

In all the exchanged samples a dependence of sorption on the ionic strength was observed -the higher the ionic strength, the lower K_d values-, but in Na-exchanged samples this dependence was not in agreement with a pure ionic exchange process. A non-negligible effect of pH on sorption was observed that could be fit considering surface complexation on the amphoteric groups present at the solid surface.

In general, results indicate that sorption of Ra in the studied clay formations is high enough to limit the radium migration in such system.

Acknowledgements:

This work has been developed in the frame of the Andra contract 062306 project “Comportement géochimique et de transfert du radium dans un contexte de stockage de déchets FAVL (Faible Activité Vie Longue)”. Ana Maria Fernandez (CIEMAT) is acknowledged for supporting analyses of clay materials.

References

Ames, L.L., McGarrah, J.E., Walker, B.A., 1983a. Sorption of trace constituents from aqueous solutions onto secondary minerals. II. Radium. Clay Clay Min. 31, 335–342.

Ames, L.L., McGarrah, J.E., Walker, B.A., 1983b. Sorption of uranium and radium by biotite, muscovite, and phlogopite. Clays Clay Min. 31 (5), 343–351.

Atun, J.C., Bascetin, E., 2003. Adsorption of barium on kaolinite, illite and montmorillonite at various ionic strengths. Radiochim. Acta 91, 223–228.

Bradbury, M.H., Baeyens, B., 1994. Sorption by Cation Exchange: Incorporation of a Cation Exchange Model into Geochemical Computer Codes. PSI Technical Report, vols. 94–07. PSI, Switzerland, p. 32.

Erten, H.N., Gokmenoglu, Z., 1994. Sorption behavior of Cs^{2+}, Zn^{2+} and Ba^{2+} ions on alumina, kaolinite and magnesite. J. Radionalytical Nucl. Chem. 182 (2), 375–394.

Eylem, C., Erten, H.N., Göktürk, H., 1990. Sorption-desorption of barium on clays. J. Environ. Radiact. 11, 183–200.

Gaines, G.I., Thomas, H.C., 1953. Adsorption studies on clay minerals: II. A formulation of the thermodynamics of exchange adsorption. J. Chem. Phys. 21, 714–718.

Gaucher, E.C., Tournassat, C., Pearson, F.J., Blanc, P., Crouzet, C., Lerouge, C., Altmann, S., 2009. A robust model for pore-water chemistry of clayrock. Geochimica Cosmochimica Acta 73 (21), 6470–6487.

Ghaemi, A., Torab-Mastaedi, M., Ghannadi-Maragheh, M., 2011. Characterisation of Sr(II) and Ba(II) adsorption from aqueous solution using dolomite powder. J. Hazard. Mater. 190, 916–921.

Giffaut, E., Grivé, M., Blanc, P., Vieillard, P., Colàs, E., Gailhanou, H., Gaboreau, S., Marty, N., Madé, B., Duro, L., 2014. Andra thermodynamic database for performance assessment: ThermoChimie. Appl. Geochem. 49, 225–236.

Görtürk, H., Eylem, C., Hatipoglu, S., Erten, H.N., 1995. Radiochemical studies of the sorption behavior of strontium and barium. J. Radioanalytical Nucl. Chem. 198 (2), 449–456.

IAEA, 2010. Analytical Methodology for the Determination of Radium Isotopes in Environmental Samples. IAEA. Analytical Quality in Nuclear Applications Series N19) IAEA/AQ/19, 2010).

Jones, M.J., Butchins, L.J., Charnock, J.M., Pattrick, R.A., Small, J.S., Vaughan, D.J., Wincott, P.L., Livens, F.R., 2011. Reactions of radium and barium with the surfaces of carbonate minerals. Appl. Geochem. 26 (7), 1231–1238.

Meier, H., Zimmerhacki, E., Zeitler, G., Menge, P., Hecker, W., 1987. Influence of liquid/solid ratios in radionuclide migration studies. J. Radioanalytical Nucl. Chem. 109 (1), 139–151.

Missana, T., García-Gutiérrez, M., 2007. Adsorption of bivalent ions (Ca(II), Sr(II) and Co(II) onto FEBEX bentonite. Phys. Chem. Earth 32, 559–567.

Missana, T., García-Gutiérrez, M., Alonso, U., 2008. Sorption of strontium onto illite/smectite mixed clays. Phys. Chem. Earth 33, S156–S162.

Missana, T., Alonso, U., García-Gutiérrez, M., 2009. Experimental study and modelling of selenite sorption onto illite and smectite clays. J. Colloid Interface Sci. 334, 132–138.

Missana, T., Benedicto, A., García-Gutierrez, M., Alonso, U., 2014. Modeling cesium retention onto Na-, K- and Ca-smectite: effects of ionic strength, exchange and competing cations on the determination of selectivity coefficients. Geochim. Cosmochim. Acta 128, 266–277.

Parkhurst, D.L., Appelo, C.A.J., 2013. Description of Input and Examples for PhreeqC Version 3 – a Computer Program for Speciation, Batch-reaction, One- Dimensional Transport and Inverse Geochemical Calculations. U.S Geological Survey, Denver, Colorado.

Shahwan, T., Atesin, A.C., Erten, H.N., Zarorsiz, A., 2002. Uptake of Ba^{2+} ions in natural bentonite and $CaCO_3$: a radiotracer, EDXRF and PXRD study.

J. Radioanalytical Nucl. Chem. 254 (3), 563–568.
Tachi, Y., Shibutani, T., Sato, H., Yui, M., 2001. Experimental and modeling studies on sorption and diffusion of radium in bentonite. J. Contam. Hydrology 47 (2), 171–186.
Tamamura, S., Takada, T., Tomita, J., Nagao, S., Fukushi, K., Yamamoto, M., 2014. Salinity dependence of ^{226}Ra adsorption on montmorillonite and kaolinite. J. Radioanalytical Nucl. Chem. 299 (1), 569–575.
Tournassat, C., Grangeon, S., Leroy, P., Giffaut, E., 2013. Modeling specific pH dependent sorption of divalent metals on montmorillonite surfaces. A review of pitfalls, recent achievements and current challenges. Am. J. Sci. 313 (5), 395–451.
Tunusoglu, O., Shahwan, T., Eroglu, A.E., 2007. Retention of aqueous Ba^{2+} ions by calcite and aragonite over a wide range of concentrations: characterisation of the uptake capacity and kinetics of sorption and precipitate formation. Geochem. J. 41, 379–379.
Van der Lee, J., De Windt, L., 1999. CHESS Tutorial and Cookbook. Technical Report LHM/RD/99/05.
Vilks, P., Miller, N.H., Felushko, K., 2011. Sorption Experiments in Brine Solutions with Sedimentary Rock and Bentonite. NWMO TR-2011-11.
Zhang, P.C., Brady, P.V., Arthur, S.E., Zhou, W.Q., Sawyer, D., Hesterberg, D.A., 2001. Adsorption of barium(II) on montmorillonite: an EXAFS study. Colloids Surfaces A Physicochem. Eng. Aspects 190, 239–249.